2-P

SQT

Department of AERONAUTICS and ASTRONAUTICS
STANFORD UNIVERSITY

NTIS HC $4.50

R. Degner
M. Kaplan
J. Manning
R. Meetin
S. Pasternack
S. Peterson
H. Seifert

THE LUNAR HOPPING TRANSPORTER

Final Report for
JULY 1971
National Aeronautics and Space Administration
Grant No. NGR 05-020-258
SUDAAR No. 428

46

SUDAAR No. 428

THE LUNAR HOPPING TRANSPORTER

by

R. Degner
M. Kaplan
J. Manning
R. Meetin
S. Pasternack
S. Peterson
H. Seifert

Final Report for

NASA Grant No. NGR 05-020-258

Department of Aeronautics and
Astronautics
Stanford University
Stanford California

July, 1971

ABSTRACT

This report describes research on several aspects of lunar transport using the hopping mode. Hopping exploits the weak lunar gravity, permits fuel economy because of partial recompression of propellant gas on landing, and does not require a continuous smooth surface for operation. Three questions critical to the design of a lunar hopping vehicle are addressed directly in this report: 1) the tolerance of a human pilot for repeated accelerations, 2) means for controlling vehicle attitude during ballistic flight, and 3) means of propulsion In addition, a small-scale terrestrial demonstrator built to confirm feasibility of the proposed operational mode is described, along with results of a preliminary study of unmanned hoppers for moon exploration.

ACKNOWLEDGMENTS

The financial support of NASA through Grant No. NGR 05-020-258 is gratefully acknowledged; the sustained interest and participation of Mr. William Larson and Mr. James Howard of NASA Ames Research Center in the study was an important element in its success. Mr. John Jones and Mr. Henry Adelman, graduate students in the Stanford Department of Aeronautics and Astronautics, made important contributions as participants in the research.

Dr. Orval Ellsworth, physiologist in private practice, and veterinarians Dr. James Parcher of NASA and Dr. James Fox of the Stanford Animal Care Facility provided technical support of numerous aspects of the animal test programs, including gross post-mortem examinations of animals and review of results thereof. At the Stanford Medical School, Dr. Klaus Lewin and Dr. Malcolm Mitchinson performed histopathological examinations of animal organs, Dr. Donald Nagel and Dr. Gerald Levine detailed examinations of animal vertebral columns, while Dr. Paul Wolf provided advice in the hematological investigations. The major contributions of all these men to the study of primate response to cyclic acceleration (Section 2) is acknowledged with thanks.

Table of Contents

	Page
Abstract	ii
Acknowledgements	iii
Table of Contents	iv
List of Figures	v
List of Tables	vi
1. Introduction	1
2. Effects of Cyclic Acceleration Pulses on Primates	4
3. Attitude Control of Hopping Vehicles	15
4. Propulsion and Ballistics	21
5. Terrestrial Prototype	28
6. Automated Hopping Devices for Lunar Exploration	35

List of Figures

Fig. No.	Title	Page
1	Parametric Design Curves for Parabolic Acceleration Pulse	13
2	Schematic Twin-Gyro Controller	16
3	Single Rotational Degree of Freedom Hardware Simulator	19
4	Experimental and Computer Results for Hardware Simulator	20
5	Schematic of Propulsion Components	22
6	Variation of Gas State Variables and Mass during Repeated Hops	26
7	Multiple Exposure of Hopper Flight Simulation Displayed on Cathode Ray Screen	27
8	Technology Demonstrator	29
9	Systems Schematic for Technology Demonstrator	30
10	Terrestrial Demonstrator in Flight	34
11	Remote Sequencing and Functions	37
12	Candidate Unmanned Hopper Configuration	39

List of Tables

Table No.	Title	Page
1.	Experimental Ride Summary	6
2.	Experimental Variables and Test Results	9

Section 1

INTRODUCTION

To date, vehicles developed for transport on the lunar surface have been wheeled, tracked, or rocket propelled. This study examines several aspects of lunar transport using the hopping mode. Hopping is attractive because it exploits the weak lunar gravity. For example, launching at 45° with a velocity of 15 ft./sec permits a horizontal leap of 50 feet in 4 sec, and launching at 45 ft./sec permits a leap of 450 ft. in 15 seconds. Use of a pneumatic piston propulsion system allows substantial fuel economy, since the propellant gas can be partly recompressed upon landing. In addition, hopping does not require a continuous smooth surface between termini, but can surmount intervening obstacles and crevasses as well as permit vertical reconnaisance hops.

Among the important questions which arise when one essays to design a hopping vehicle are (a) the tolerance of a human pilot for repeated accelerations, (b) means for controlling vehicle attitude during ballistic flight, and (c) means of propulsion. Two questions which are omitted from this report are the foot-soil interaction during acceleration, and acquisition of target point coordinates. Although the original hopper or lunar "Pogo" concept [1]* envisaged take-off at 1 earth g along a 30-ft. pole, later desire to have a vehicle small enough to be carried on Apollo resulted in the arbitrary decision to study a small hopper which accelerated at an average value of 3 earth g's through a 2-foot displacement only, permitting 50-foot hops. Subsequent work on the acceleration tolerance of primates indicates that this displacement should probably be increased by a factor of two or three, with corresponding reduction in peak acceleration, to provide a satisfactory ride for humans.

---

* Numbers in brackets indicate references listed at the end of this report.

The model chosen for attitude control during flight utilized three sets of twin gyros which during flight could exchange angular momentum with the vehicle around any of three orthogonal axes. Two operational modes were considered: (a) pilot and vehicle at fixed horizontal attitude with propulsion leg rotation 90° during flight from launch to landing orientation, and (b) propulsion leg fixed to the vehicle, with entire ensemble, including pilot, rotating during flight to the landing orientation. The latter option was chosen for analysis and simulation since it was mechanically less complex and resulted in the pilot's acceleration forces remaining fixed in his body axes.

The propulsion system model comprised a piston and cylinder attached to a "foot" broad enough to stabilize angular motion around an "ankle" while the vehicle rested on the lunar surface. Specified range was achieved by careful adjustment of initial pressure in the cylinder. The energy losses resulting from impact of the foot upon landing were made up by adjustment of the mass of gas in the cylinder.

To confirm the hopping concept, a small-scale terrestrial demonstrator was built which used 2000 psia cold nitrogen as propellant and was stabilized passively about a vertical axis by a single gyroscope. For simplicity, pneumatic shock absorbers were used for landing rather than re-orientation of the propulsion leg. This vehicle was able to perform about 20 ten-foot hops per filling of its N_2 bottles. These were equivalent to 60-foot lunar hops.

In view of the limited Apollo program, preliminary study has been given to the possibilities of unmanned hoppers on the moon. Because of the absence of a pilot, such vehicles could use much greater acceleration and be correspondingly compact. They would, however, require much more sophisticated guidance systems, and if controlled by earth-based operators, be subject to the 1.5 second one-way time delay in execution of commands. A possible operational plan for such an unmanned device is discussed in the final section.

All of the work described in this report was carried out in fulfillment of degree requirements by graduate students at Stanford

University with the support of NASA; previous reports on this work include [2 through 6]. Of the work reported here, the study of effects of acceleration on primates was done by R. Degner, the attitude control system by S. Pasternack, the propulsion analysis by R. Meetin, the terrestrial demonstrator by S. Peterson, and the unmanned system by M. Kaplan. General supervision of the work was shared by H. Seifert and J. Manning.

Section 2

EFFECTS OF CYCLIC ACCELERATION PULSES ON PRIMATES

Introduction

The major consideration for selecting an acceleration profile for a manned vehicle must be "Can the pilot take it?" Although earlier ballistics and propulsion analyses had been carried out [3] assuming take-off and landing acceleration pulses of 5 g maximum (3 g average) and 0.2 seconds duration, it had not been established that a human could withstand very many cycles of this acceleration profile.

There have been no previous studies of the effects on humans of cyclic acceleration pulses of the type encountered in hopping vehicle operation or of the basic way in which the design of a hopping vehicle is affected by its acceleration profile. An investigation of these matters was therefore undertaken; this study proved so challenging and its results so significant that it became the principal focus of dissertation research [7]. This study has involved the following three areas: design and construction of a cyclic acceleration facility, an experimental investigation of cyclic acceleration tolerance, and an analytical study based on a mathematical model.

Cyclic Acceleration Facility

No acceleration test facility was available which could be programmed to produce cyclic acceleration pulses, so a facility was designed and constructed. There were not sufficient funds available to build a general-purpose facility with active control of the pulse shape. Instead, a special-purpose facility capable of generating cyclic acceleration pulses of 0.2 seconds in width and up to 5 g in magnitude with passive control of the pulse shape was designed and constructed.

The basic principle of the design is to reel a guided impact assembly upward with a drive train to some height, disengage the cable takeup spool from the rest of the drive train which allows the impact assembly to

accelerate downward under the influence of gravity, and stop the impact assembly with a hydraulic-pneumatic shock absorbing system mounted onboard.

Three standard drop heights of 32, 50 and 68 inches were used during operation of the facility. Friction and drag limit the free-fall acceleration to about 0.8 g which results in impact velocities of approximately 10.8, 13.9, and 16.5 ft/sec, respectively for the three drop heights. Maximum accelerations are 2.6, 3.8, and 5.0 g with a pulse width of about 0.2 seconds in all cases. A three speed transmission in the drive train gives three cable takeup speeds. The three cable takeup speeds coupled with three drop heights result in nine standard rides used in the experimental tests. The rides are summarized in Table 1.

Experimental Investigation

The original plan for this study was similar to that used in previous studies of human tolerance to acceleration inputs, i.e., to start with low acceleration intensities and short exposure times and then to increase both up to the limit of human tolerance based on subjective reaction. A test protocol which included the plan to use human subjects was submitted to the Stanford University Committee on the Use of Human Subjects in Research. However, this Committee recommended preliminary animal tests since this type of acceleration input had never been previously used with either animal or human test subjects.

Monkeys were selected for this study because of their anatomic and dynamic similarity to humans. These animals are dynamically similar to humans in that [8]:

1) the major resonance of both is centered in the abdominal and thoracic viscera
2) the major resonance occurs at approximately 5 Hz in both primates
3) the major resonance is damped approximately equally in both.

The test animals ranged in weight from 12 to 20 pounds. A harness was used to restrain the animals in a seated position but was not so tight as to appreciably affect their dynamic response. The only padding used was 1/4 inch felt on the seat so that the accelerations measured on

the impact assembly were very nearly the same as those input to the seat of the animal.

The animals were exposed to rides in order of ascending number (see Table 1). Each ride was continued for 1 hour, then a rest period of several hours was used before the next ride was input to the animal. No more than two hours of exposure was given to any one animal on one day. In most cases, the animals were subjected to rides on successive days.

All of the animals were x-rayed before their first exposure and after their last to check for dislocated or fractured bones. In nearly all of the tests, the animals were sacrified 12 to 24 hours following their most intensive acceleration exposure. An autopsy was performed on each animal and all of the organs sent to a pathologist for microscopic examination. The spine is the most heavily loaded part of the skeleton, so it was excised in several animals and sent to an orthopedic surgeon for detailed examination.

Ride No.	Impact Vel.	Max. Accel.	Cycles/Hour
1	10.8 ft/sec	2.6 g	380
2	10.8 ft/sec	2.6 g	640
3	10.8 ft/sec	2.6 g	820
4	13.9 ft/sec	3.8 g	290
5	13.9 ft/sec	3.8 g	490
6	13.9 ft/sec	3.8 g	640
7	16.5 ft/sec	5.0 g	230
8	16.5 ft/sec	5.0 g	400
9	16.5 ft/sec	5.0 g	510

Table 1. Experimental Ride Summary

Table 2 summarizes the test variables and results of the experimental study. Some negative results were obtained with the first three animals tested so the study was extended to include four additional animals. Monkey X-4 was used for both tests I and VIII.

The first two tests yielded little data since both animals were held for long post-test recovery periods. In the remaining test, however, all of the animals were sacrificed 12 to 24 hours post-test. For all six of these tests, there was no evidence of pathology during the pre-autopsy observation period. There was some soft tissue damage in a couple of the tests (III and VII) but this was of a minimal to moderate degree and certainly not life-threatening.

The pathologists concluded that the most serious hazard to the animals undergoing exposure to the accelerations was fat embolism. None of the three animals exposed to only the first six rides (Tests V, VI, and VIII) contracted this disorder. However, all three of the animals exposed to total exposures of greater than eight hours (Tests III, IV, and VII) had varying degrees of fat embolism.

No attempt will be made to cover all of the various aspects of fat embolism in this discussion. For a more thorough discussion than that given here, the reader is referred to a recent paper by Levy[9] which deals in some detail with the pathogenesis, diagnosis, treatment, and prognosis of fat embolism.

Embolism indicates the sudden blocking of an artery or vein (or capillary) by a clot or obstruction, which has been brought to its place by the blood current. Fat embolism is a disorder wherein fat droplets of size sufficient to occlude or block the small blood vessels of the various organs in the body appear in the circulating blood. It is a frequent and often serious complication in individuals who have been injured. Although fractured bones are the commonest clinical association of fatal fat embolism in man, there is ample evidence that concussion of bones without fracture, and soft tissue injury, can lead to fat embolism.

The exact mechanism behind the formation of fat emboli is not known. However, the mechanical theory is the most widely accepted. According to the mechanical theory, injury to tissues containing fat cells, such

as bones and soft tissues, ruptures the cells, releasing the fat in droplet form. At the same time, the capillaries and small veins draining the injured tissue are disrupted, resulting in the entry of the fat droplets into the vascular channels.

Fat embolism kills because it impairs the function of many organs in the body, particularly the lung and brain, by interrupting their blood supply. It is potentially a very serious disorder in that:

1) minimal trauma can cause the formation of fat emboli
2) definitive diagnosis by clinical tests is very difficult
3) an asymptomatic period varying from minutes to hours following injury makes tentative diagnosis difficult
4) in the seriously ill patient with fat embolism, the mortality rate is near 100% without therapy.

The finding that fat embolism was the main hazard to the animals undergoing this experiment is remarkable in that no studies on acceleration tolerance were found in the literature in which fat embolism was listed as a primary or even secondary hazard. This is somewhat more remarkable when one considers that, even though fat embolism is always secondary to injury or certain other diseases, an Austrian study [9] of 263,861 injury cases in which 5,265 of the patients died found fat embolism to be the primary or a contributing cause of death in 16% of the cases.

More animal experiments would have been very desirable to further establish what combinations of exposure time and acceleration levels produce fat embolism. However, the large amount of time and support needed to conduct an extensive experimental program of this nature was not available.

Analytical Study

The objective of the experimental study was to determine whether humans could tolerate cyclic acceleration pulses of approximately 0.2 seconds in duration and 5 g's in magnitude. However, the preliminary animal experiments indicated the potential danger of subjecting human subjects to these types of accelerations.

EXPERIMENTAL VARIABLES								TEST RESULTS						
								Pre-Autopsy Observations			Autopsy and Histological Findings			
Test	Monkey	Adult Age	Physical Condition	Total No. of Test Cycles	Max. Accel. Exposure	No. Test Days / No. Rest Days	Post-Test Recovery	Distress During Test	Post-Test Disability	X-Ray Fractures or Dislocations	Soft Tissue Damage	Retinal Detachment	Fat Emboli	Blood Damage or Discase
I	X-12	old	sedentary	4,910	5.0 g	6/9	15 days	neg	neg	neg	neg	---	neg	pos
II	X-4	old	sedentary	4,910	5.0 g	6/5	10 mos.	neg	neg	neg	Held for long-term x-ray study			
III	X-32	old	sedentary	4,620	5.0 g	5/1	13 hrs.	neg	neg	neg	pos	---	pos	---
IV	R-107	young	active	4,860	5.0 g	5/0	12 hrs.	neg	neg	neg	neg	neg	pos	neg
V	M-386	old	medium	3,260	3.8 g	3/0	23 hrs.	neg	neg	neg	neg	---	neg	?
VI	X-405	middle	active	3,260	3.8 g	3/0	20 hrs.	neg	neg	neg	neg	---	neg	neg
VII	A-38	young	active	3,890	5.0 g	4/0	17 hrs.	neg	neg	neg	pos	---	pos	neg
VIII	X-4	old	sedentary	3,515	3.8 g	4/0	24 hrs.	neg	neg	neg	?	---	neg	neg

Key: --- - Examination not performed
neg - Negative findings, no evidence of pathology
pos - Positive findings, evidence of pathology
? - Questionable findings, suggestive but not conclusive

Table 2. Experimental Variables and Test Results

Since the acceleration profile plays such a basic role in the design of a manned hopping vehicle, an analytical investigation of human tolerance to various acceleration inputs was initiated. This study was based on the use of a mathematical model to describe human dynamics and had two phases: 1) use the acceleration curves from the experimental study and input them to the model to predict human tolerance, and 2) using functional acceleration inputs, study the effects of different pulse widths and cyclic frequencies on human tolerance.

The mathematical model used in this study was developed by a group [10] at the U.S. Army Tank-Automotive Command using experimental transfer function techniques. They found that a human could be modeled as a quasi-linear spring-mass-damper system for inputs below the limit of human tolerance.

In the frequency domain, the acceleration input to a human can be represented by its power spectral density or in the case of a periodic function, by its Fourier series. However, a description of the acceleration inputs fails to identify human response to the input. The Army group, based on experimental tests with both sinusoidal and random inputs, found that subjective discomfort correlates directly to the average amount of power absorbed internally. Their expression for the average absorbed power P_{av} in the frequency domain is:

$$P_{av} = \sum_{i=1}^{N} K_{it} A_i^2 rms$$

where K_{it} = frequency dependent parameter which describes dynamics of a seated human

$A_i^2 rms$ = mean squared acceleration components at frequency f_i

Ambient parameters such as vision, audition, motivation, and mental set or expectancy can drastically influence a subject's response to his vibration environment. For these reasons, it is difficult to even suggest a desirable limit of average absorbed power. However, the Army group found that a 10 watt ride was voluntarily endured for approximately only one minute. Therefore, it seems that if a ride is to be tolerated for more than a few minutes, it must be sufficiently smooth such that P_{av} is well below 10 watts.

For the analytical study, all of the calculations necessary to obtain P_{av} from the acceleration input were performed on a digital computer. The experimental acceleration rides were taped on an analog tape recorder, the data A-D converted, and the samples stored on digital tape. The Fourier coefficients were obtained using a library subroutine and the mean squared acceleration at a given frequency computed from the coefficients at that frequency.

The nine experimental rides gave values of P_{av} ranging from approximately 6 to 21 watts in a fairly even fashion. These results indicate that a human would not tolerate any of the experimental rides for more than a few minutes.

With respect to the experimental rides, it was also noted that even though the major forcing components were below 2 Hz in all cases, those frequency components which contributed most to P_{av} were at approximately 4 Hz. In other words, if the experimental rides were inputted to a human, most of the absorbed power would be dissipated in the thoracic and abdominal viscera. Since monkeys are dynamically similar to humans, the fat embolism in the animals was likely caused by repeated damped oscillations of the thoracic and abdominal viscera which were forced by the acceleration input pulses.

The second phase of the analytical study was carried out using functional acceleration inputs to see if any pulse was better than that used in the experimental investigation. In order to maximize the utility of this investigation as regards the design of a hopping vehicle, the periodicity of the acceleration pulses was made to coincide with a simplified dynamic model of a hopping vehicle in a lunar environment. The vehicle was modeled as a point mass launched and landed at 45° with respect to level terrain. All losses were neglected so that the model ballistic flight was parabolic in shape and the landing was a mirror image of the takeoff.

A parabolic shape was used for the landing and takeoff acceleration pulses. Three independent variables, acceleration pulse width t_{pw}, height g_{max}, and the time interval between landing and the subsequent takeoff t_{rest}, serve as inputs to the dynamic vehicle model. All of the

remaining parameters which characterize flight are dependent variables and can be calculated from these three inputs. The most important dependent variables from a design standpoint are the stroke required for takeoff d_{to}, the horizontal distance covered in one hop d_{hop}, the total time per cycle t_{cycle}, and the average ground speed v_{av} (equals d_{hop}/t_{cycle}). In addition, P_{av} was calculated for each acceleration profile by inputting the waveform into the dynamic human model.

Fig. 1 gives parametric design curves for use in hopping vehicle design. Even though they are dependent parameters, the average ground speed v_{av} and average absorbed power P_{av} are the most important variables so they were used for the major axes. One independent variable t_{rest} was held constant at 5 seconds. Computer runs were made with t_{pw} held constant and g_{max} incremented in steps of 1 g. The takeoff stroke d_{to} is also a very important parameter from a design standpoint so lines of constant stroke distance were mapped on the original curves.

From an inspection of the parametric design curves, a number of interesting observations are immediately apparent. For instance, assume that 8 ft/sec is the minimum average ground speed that would prove useful for a lunar hopping vehicle. This speed can be accomplished by using a parabolic pulse with $t_{pw} = 0.2$ sec and $g_{max} = 5g$. However, this results in an average absorbed power of over 30 watts, well above the 10 watt maximum which can be tolerated for any length of time. The same average ground speed can be effected by using a pulse with $t_{pw} = 0.5$ sec and $g_{max} = 2$ g. This pulse gives an acceleration profile for which P_{av} is approximately 2 watts! The penalty for going from the former ride to the latter is an increase in the takeoff stroke d_{to} from approximately 2 feet to approximately 6 feet.

The explanation for marked decreases in P_{av} and hence subjective discomfort for the same average ground speed with wider pulse widths can be summarized as follows. Pulse widths of approximately 0.2 seconds give acceleration profiles with significant components in the region of 5 Hz, which are particularly intolerable in that they excite the major visceral resonance. In general, the wider the pulse width, the lower the frequency components of the associated ride, which produces less subjective discomfort for the same average ground speed.

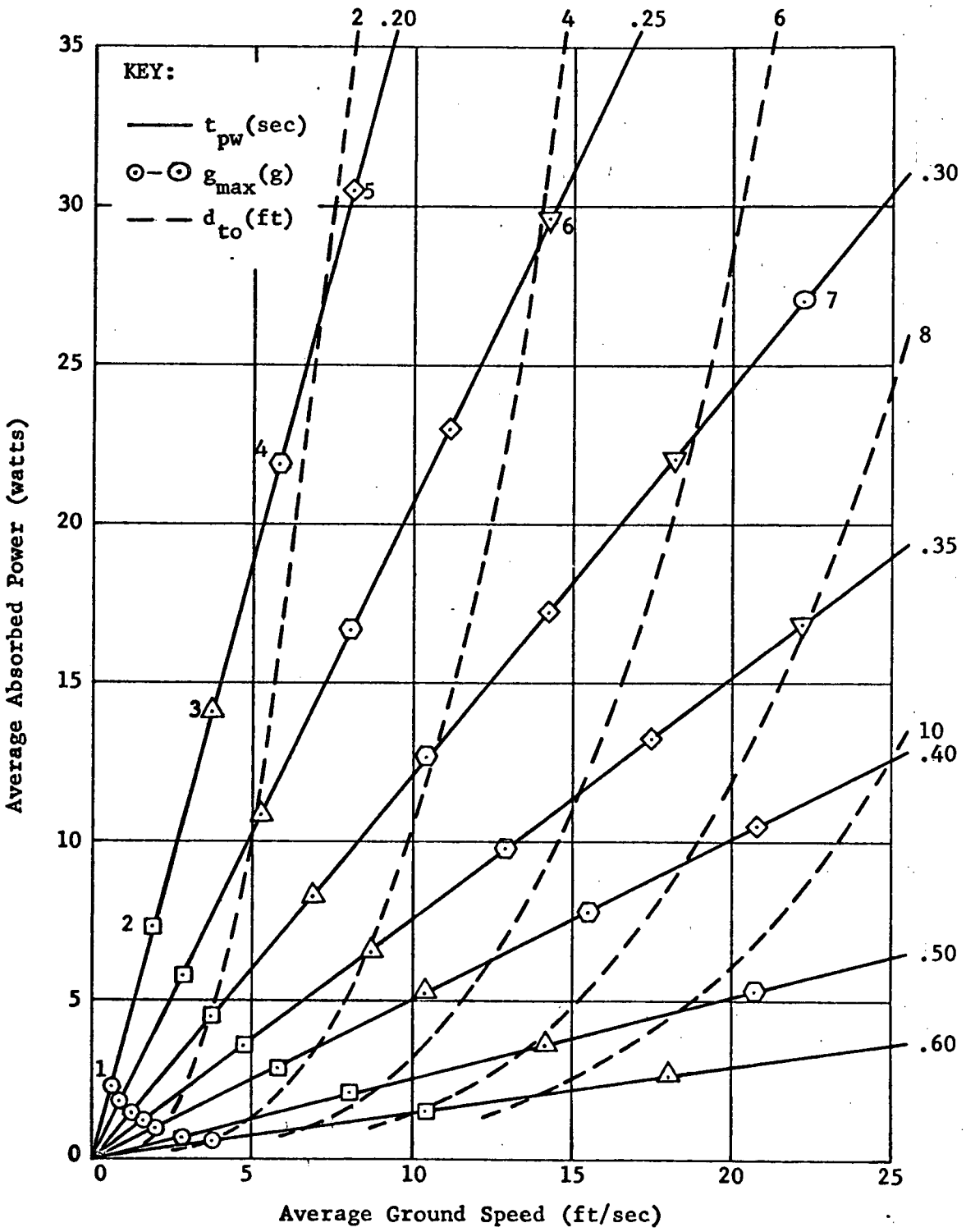

Figure 1. Parametric Design Curves for Parabolic Acceleration Pulse
t_{rest} = 5.0 sec

Conclusions and Recommendations

Fat embolism was found to be the main hazard to animals exposed to cyclic acceleration pulses. However, fat embolism is most commonly clinically associated with injuries resulting from single impacts. This suggests that fat embolism is at least a secondary hazard for a wide range of acceleration exposures and this premise should be explored with further animal studies. In addition, the findings of the experimental study raise serious questions regarding the common practice in studies of human voluntary tolerance of progressively increasing the acceleration loading and/or exposure time to the point where subjects complain of moderate to severe pain.

The analytical study indicated that a human could tolerate the ride of a hopping vehicle at speeds of at least 8 ft/sec if pulse widths of at least 0.4 sec were used. These results should be verified by experiments involving first monkeys to check for fat embolism and other hazards and then continuing with human subjects if warranted.

Section 3

ATTITUDE CONTROL OF HOPPING VEHICLES

In this section, the automatic attitude control of hopping vehicles is analyzed assuming the use of paired control moment gyros to produce torques on the vehicle. The analyses are verified both by computer and hardware simulations. A more detailed discussion of the subject matter of this section is given in [11].

After a hopping vehicle leaves the surface, it must be reoriented so that the propulsion leg is at the instant of landing nearly aligned with the mass center velocity vector. Upon landing, the vehicle is rotated to the vertical and this orientation is maintained until the initiation of the next hop. The rotations at take-off and landing may be accomplished by precessing control moment gyros in a paired or twin configuration (Fig. 2). In such a configuration, moments are produced about a single body axis much like flywheel attitude control systems. Momentum storage devices such as control moment gyros are attractive for use in hopping vehicles because no mass is expelled on each hop as would be the case for rocket reaction systems.

The magnitude of angular momentum which must be stored in the twin gyro controller is determined in part by the flight time during which the vehicle must be rotated from the launch to landing orientation. Minimizing the amount of this stored angular momentum is accomplished by allowing gyro gimbal angles to approach 90°, at which angle all of the stored angular momentum is transferred to the vehicle. If large gimbal angles are to be achieved, the torque motor which precesses the gyros must have a torque capability greater than 0.71934 of $2h^2/I$, where h is the angular momentum of each gyro rotor and I is the moment of inertia of the vehicle about its pitch axis. This relationship results from the intimate coupling of the gyro and vehicle equations of motion. Unlike flywheel attitude control systems, all of the stored angular momentum in a twin-gyro controller cannot be transferred to the vehicle with an arbitrarily small torque level.

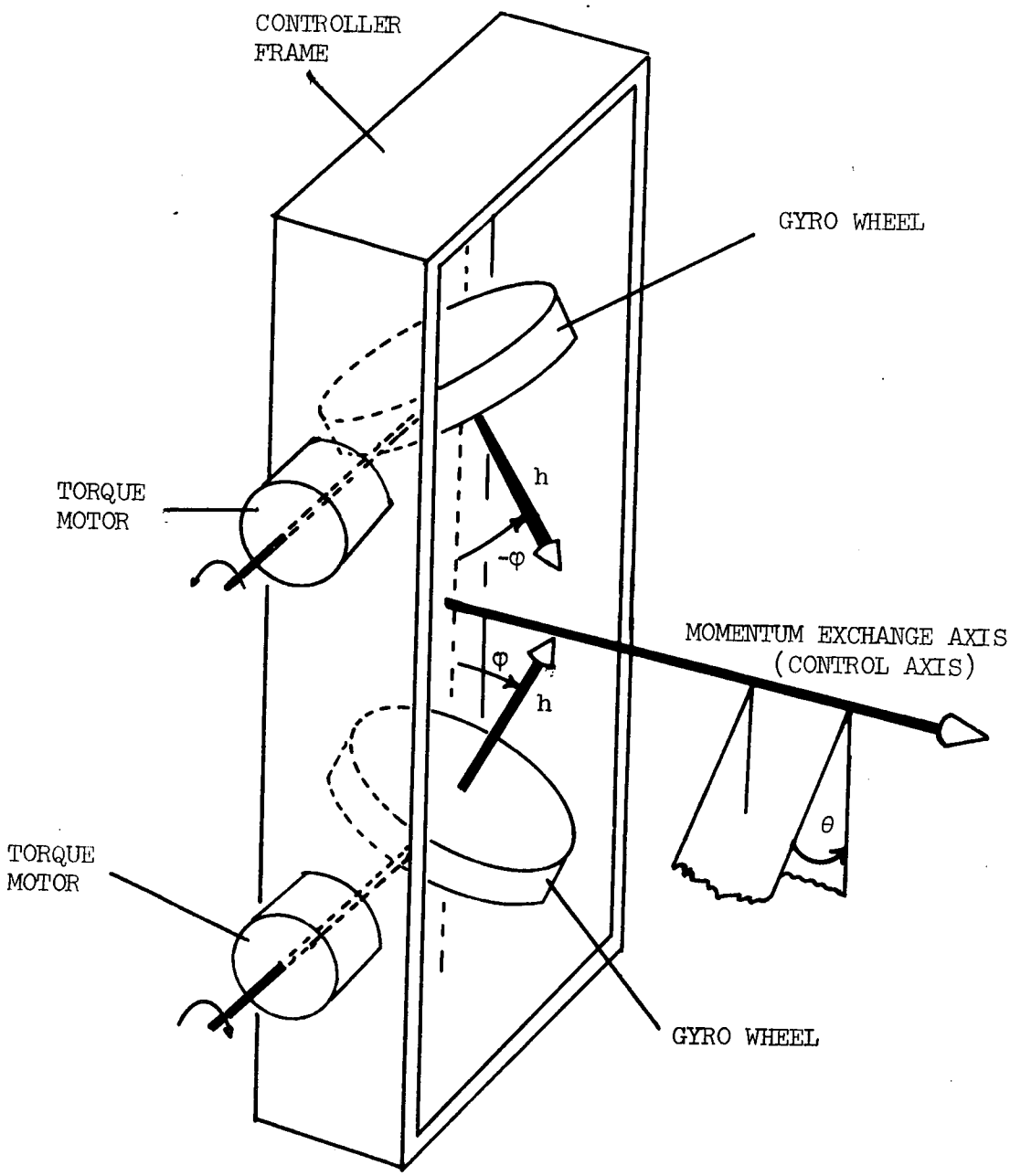

Figure 2. Schematic Twin-Gyro and Coordinates

To use the stored angular momentum most efficiently requires an optimum control torque strategy. The strategy which minimizes the time required to rotate the vehicle from the launch to landing orientation is bang-bang in nature, i.e., the torque motor should always operate at its maximum positive or negative value of output torque. Allowing a gimbal angle of 90° results in a singular solution to the optimal equations for which the control strategy is zero torque. In this case, a gimbal angle of 90° is an equilibrium angle requiring no torque from the motor. Clearly, a gimbal angle of 90° places the vehicle upon a minimizing singular arc since all of the stored angular momentum has been transferred to the vehicle. The times during the reorientation maneuver when the torque switches sign or becomes zero are determined by solving a two-point boundary value problem for which the equations are nonlinear. The solution obtained is open loop, i.e., the desired terminal conditions will be met only if the initial conditions are known precisely and if the mathematical model adequately describes the system. A sub-optimal control law which is easily realizable may be formulated for response to an initially large error as follows: an initial period of maximum torquing when error is large is followed by a period in which torque is proportional to the state variables, which insures meeting the terminal conditions. Such a control law has been implemented in the hardware simulator.

An actual hopping vehicle with six degrees of freedom must have three twin-gyro controllers, each one controlling about a single body axis. The roll and yaw controllers must align the vehicle pitch axis with the normal to the plane formed by the mass center velocity vector and the direction of gravity. As the vehicle rotates about the pitch axis to the landing orientation, the roll and yaw controllers must continually exchange angular momentum to reduce errors associated with any initial angular momentum contained in the roll-yaw plane. The control laws for the three twin-gyro controllers have been verified by digital simulation.

The analysis of a single rotational degree of freedom vehicle has been demonstrated by means of a hardware simulation. The vehicle, pictured in Fig. 3, is constrained to have but one rotational degree of freedom by floating the vehicle on a thin cushion of gas above a smooth table. In this way, the vehicle can translate in the plane of the table with frictional forces and moments reduced to a low level.

By tilting the table, a component of gravity is obtained within the plane of the table allowing the vehicle to hop and land by pushing against a ledge at the lower edge of the table. The simulator vehicle is self-contained, carrying its own gas supply for support, batteries for electrical power, and sensors and electronics for implementation of the various control laws. The vehicle attitude angle is measured by a low friction potentiometer coupled to a two-degree-of-freedom directional gyro. The only other directly measured parameter is the twin-gyro controller gimbal angle. These signals are processed in the electronics package and a voltage is applied to the controller torque motor. The vehicle attitude and gimbal angle signals are also brought to an external strip recorder by means of a light, flexible umbilical wire for recording. The data from the simulator vehicle have been compared with the digital simulation and the agreement is very good (see Fig. 4).

The analyses and simulations have shown that twin-gyro controllers are well suited to the attitude control problems associated with hopping vehicles.

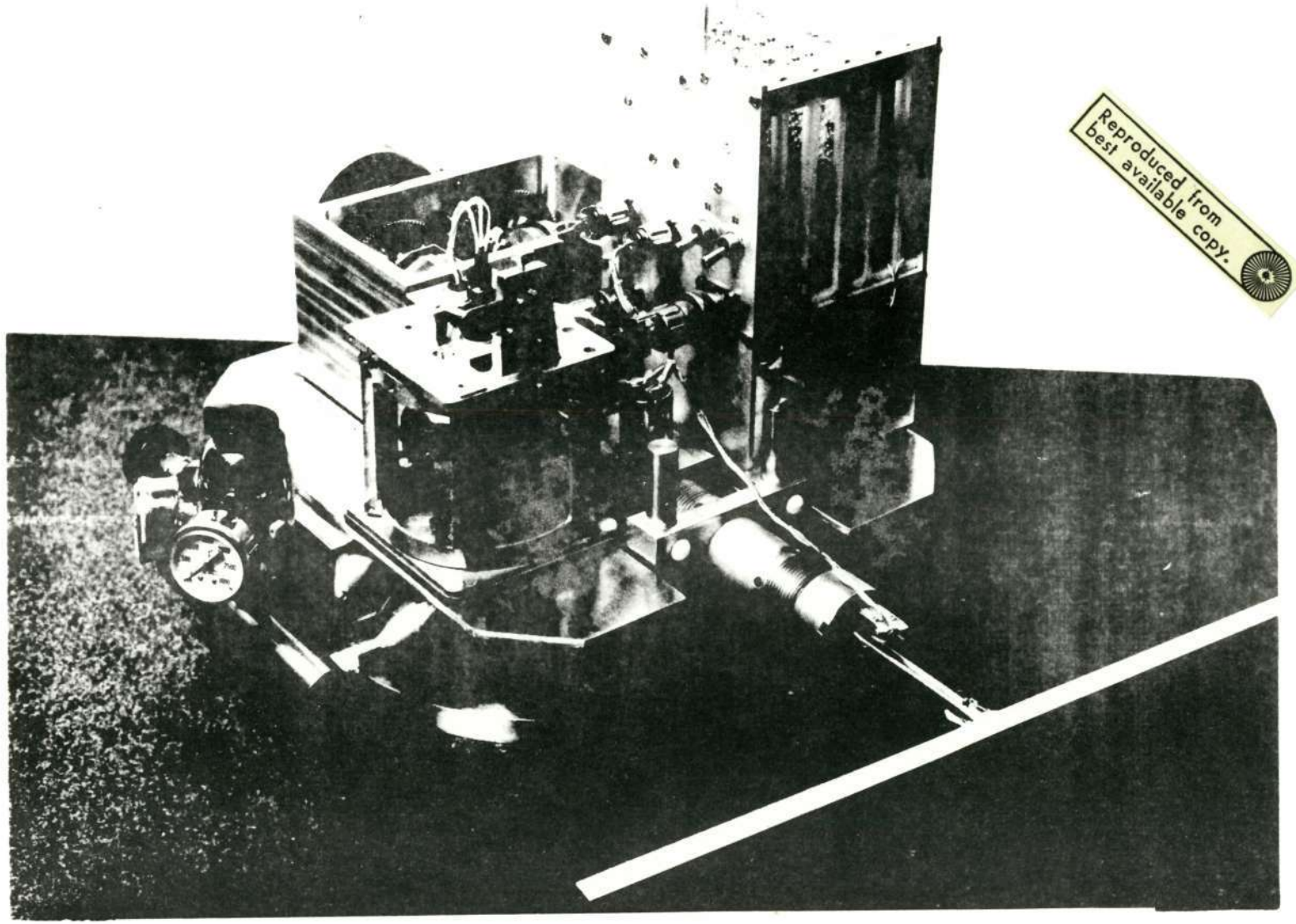

Figure 3. Single Rotational Degree of Freedom Hardware Simulator

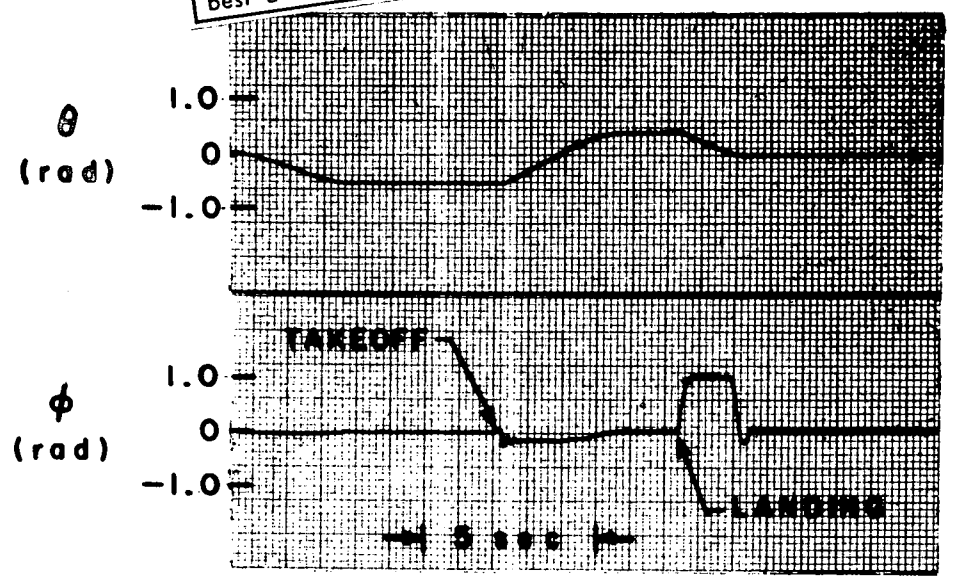

TYPICAL HOP DATA

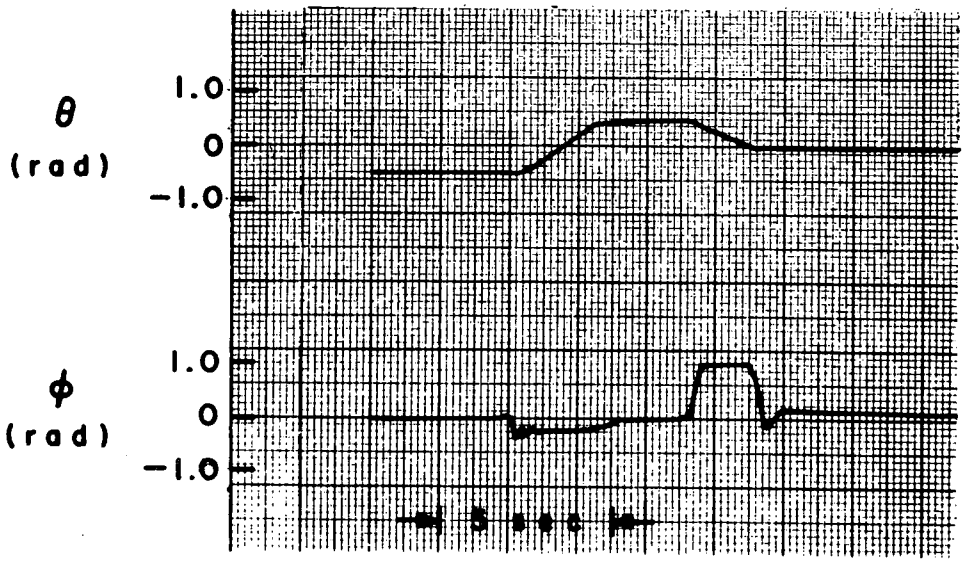

DIGITAL COMPUTER SIMULATION. NOTE GOOD AGREEMENT BETWEEN THE ACTUAL HOP AND DIGITAL SIMULATION DATA.

Figure 4. Experimental and Computed Results for Hardware Simulator

Section 4

PROPULSION AND BALLISTICS

Introduction

The propulsion unit for the lunar hopper imparts a specified velocity to the vehicle at take-off and, assisted by the control system, decelerates it to zero velocity at landing. Considered along with the ballistic motion must be possible on-ground motion between hops. Initial ballistic analysis was done by Seifert and Kaplan [1,2,3]. The work described in this section is presented in more detail in [12].

Design

A gas-piston system was selected for primary propulsion. Fig. 5 shows schematically the important propulsion components for a hopper using a propulsion leg fixed to the vehicle. The accumulator provides high-pressure gas to the cylinder. Pressure adjustments are made by adding gas to or venting gas from the cylinder to the lunar vacuum. The propellant gas supply unit includes tanks and other necessary hardware. A leg brake controls (i.e., decreases) the relative velocity between the leg and main body. In addition, an ankle brake at the pivot controls the relative angular velocity between the foot and leg.

In normal operation, the vehicle is initially on the ground with the leg oriented vertically. The pilot sets the desired launch azimuth, horizontal range, and launch angle into the system to initiate the hop. The vehicle rotates about the vertical to the launch direction and then tilts to the launch angle. The cylinder pressure is adjusted to a predicted initial value. The gas in the cylinder expands, forcing the main body to accelerate up the leg. (The foot may slide somewhat along the ground.) The control system monitors the main body velocity. When a specified velocity is reached, the leg brake rapidly "engages" or picks up the leg.

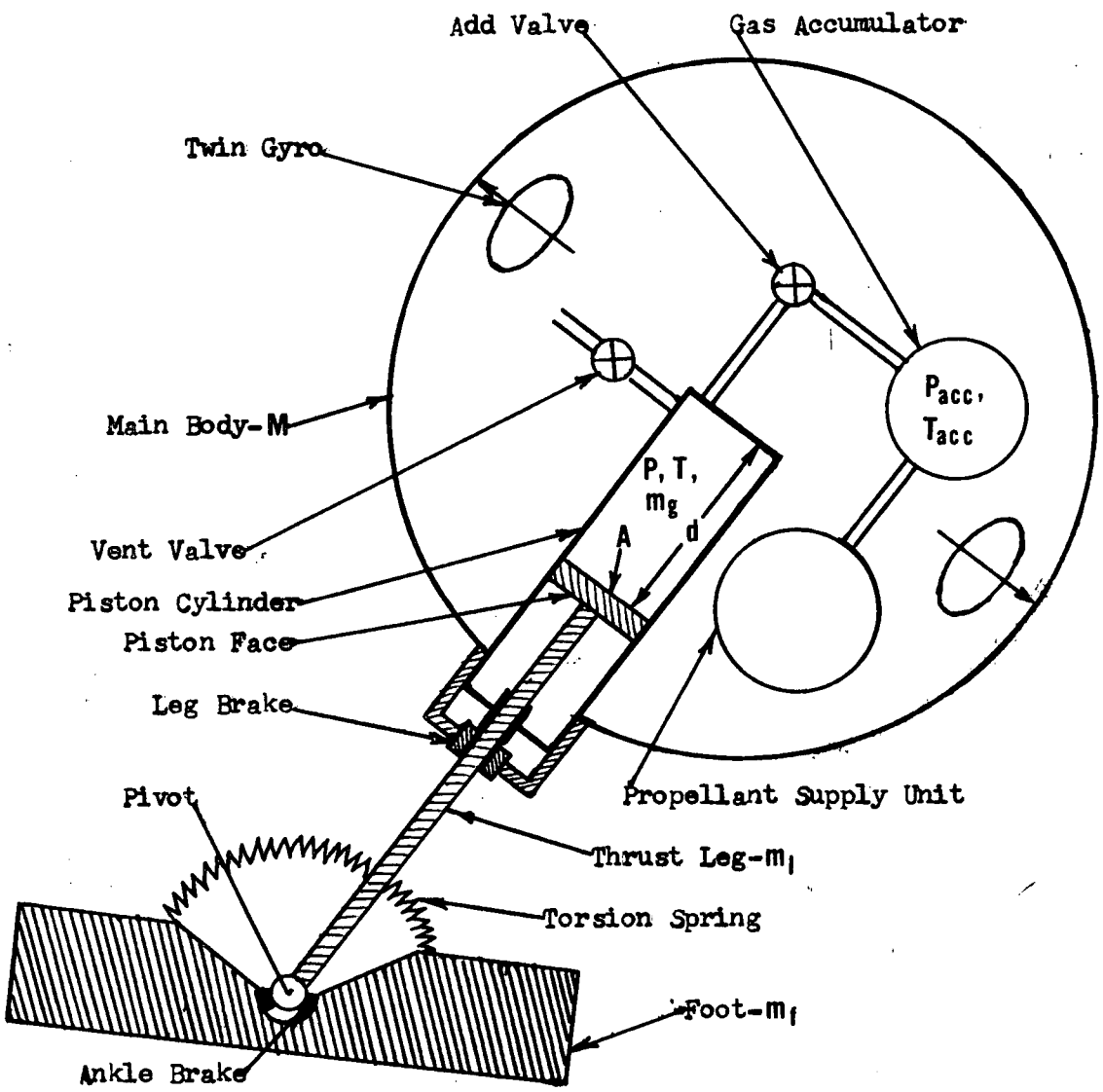

Figure 5. Schematic of Propulsion Components

During the free flight, the vehicle follows a ballistic parabola. Free flight ends as a part of the foot touches down on the ground. The foot then may "slap down" toward the ground. During free flight or slapdown the cylinder pressure may be readjusted. As the entire foot impacts the ground, the leg brake releases to disengage the leg from the main body. The main body decelerates down the leg, recompressing the gas. Simultaneously, the vehicle rotates toward the vertical. The foot may again slide. When the relative velocity between the main body and leg reaches zero, the leg brake locks. Shortly afterwards the ankle brake locks as the vehicle reaches the vertical to end the hop.

Propulsion operation is partially conservative because much of the energy expended by the gas during acceleration is recovered at deceleration. However, pressure adjustments in the cylinder by adding and venting gas must generally be accomplished to account for energy losses (e.g., engagement) and elevation changes.

Either a cold (non-reacting) gas or a hot (reacting) gas could be used in the propulsion unit. Possible cold gases include air, He, H_2, NO, N_2, and O_2. A cold gas system using N_2 was chosen for analysis of this model. A likely candidate for a hot gas system is hydrazine (N_2H_4), which decomposes catalytically or thermally into gaseous ammonia, nitrogen, and hydrogen.

Flight Analysis

To estimate ideal vehicle performance, a frictionless, non-sliding model of the propulsion and ballistics has been formulated. Assuming isentropic gas expansion and instantaneous leg braking, the first-order equations of motion for acceleration, free flight, and deceleration were derived. Using the free-flight equations, the optimum launch angle which maximizes the range is found to be $\alpha_{opt} = 45° + \sigma/2$, where σ is the average surface slope. Specializing to α_{opt}, for $-10° \leq \sigma \leq 10°$, approximate analytical solutions with a numerical error of less than 1% have been found for the initial and final cylinder pressures p_o and p_f :

$$p_o = \frac{(\gamma - 1)(M + 2m)g}{2A\left[1 - \left(\frac{d_o}{d_e}\right)^{(\gamma - 1)}\right]} \frac{X_R}{d_o} \tan \alpha_{opt}$$

$$p_f = \frac{(\gamma - 1)\, Mg}{2A\left[1 - \left(\frac{d_f}{d_d}\right)^{(\gamma - 1)}\right]} \frac{X_R}{d_f} \cot \alpha_{opt}$$

where X_R = horizontal displacement of vehicle, M and m are vehicle and leg mass, γ is gas specific heat ratio, g the lunar gravity, and A the piston area. The subscripted d's indicate start and stop positions of the piston for the expansion and compression strokes. Equations for the amount of gas to be added and vented have also been derived.

Fig. 6 shows the thermodynamic variations in cylinder pressure, temperature, and gas mass for a typical level, uphill, and downhill hopping sequence, cyclically repeated. The parameters for this sequence are:

M = 37 slug	$d_o = d_f = 1$ ft
m = 3 slug	$d_e = d_d = 3$ ft
T = 530°R	$\gamma = \gamma(N_2) = 1.40$
X_R = 50 ft	g = 5.31 ft/sec^2

The solid lines in Fig. 6 show the "equilibrium" thermodynamic cycle (for three hops) approached as the number of hops in the sequence becomes very large. Using this sequence, the equilibrium consumption for 1000 hops at 50 ft per hop (10 miles) is 0.8 slug of cold N_2. To this amount an allowance of 75 to 100% is added to account for non-optimum launches, rougher terrains, refillings if necessary, ullage, and a safety reserve. The total N_2 required for the 10-mile trip is estimated to be 1.5 slug. If N_2H_4 were used, 0.3 slug of fuel would be needed for the same trip.

Second-Order Model

To obtain a more realistic estimate of the vehicle performance, a second-order model of the propulsion and ballistics was established. It included realistic effects such as sliding, friction at the pivot and in the piston, rotation during deceleration, and non-instantaneous engagement. The effects of the leg brake, ankle brake, propellant-feed system, gyro-control system, and foot-control mechanism were considered and a prediction model for cylinder pressures was used.

The resulting nonlinear equations were organized into a computer program for numerical integration. Solutions were obtained for about 80 different hop configurations within the following ranges of hop parameters:

Average surface slope:	$-20° \leq \sigma \leq 20°$
Desired horizontal range:	$30 \text{ ft} \leq X_R \leq 60 \text{ ft}$
Static coefficient of friction:	$0.67 \leq \mu_{stat} \leq 2.00$
Kinetic coefficient of friction:	$0.33 \leq \mu_{kin} \leq 1.20$

Analysis of hopper landings indicated that rather large valves may be needed to vent gas as fast as is necessary. Also, a small amount of sliding during take-off (i.e., 3 in to 6 in) can have a large effect on performance.

To provide a better picture of the proposed hop configurations, a computer-graphical display of the second-order model doing a hop in real time was set up; results were recorded on motion picture film. Fig. 7 shows a multiple exposure of this display.

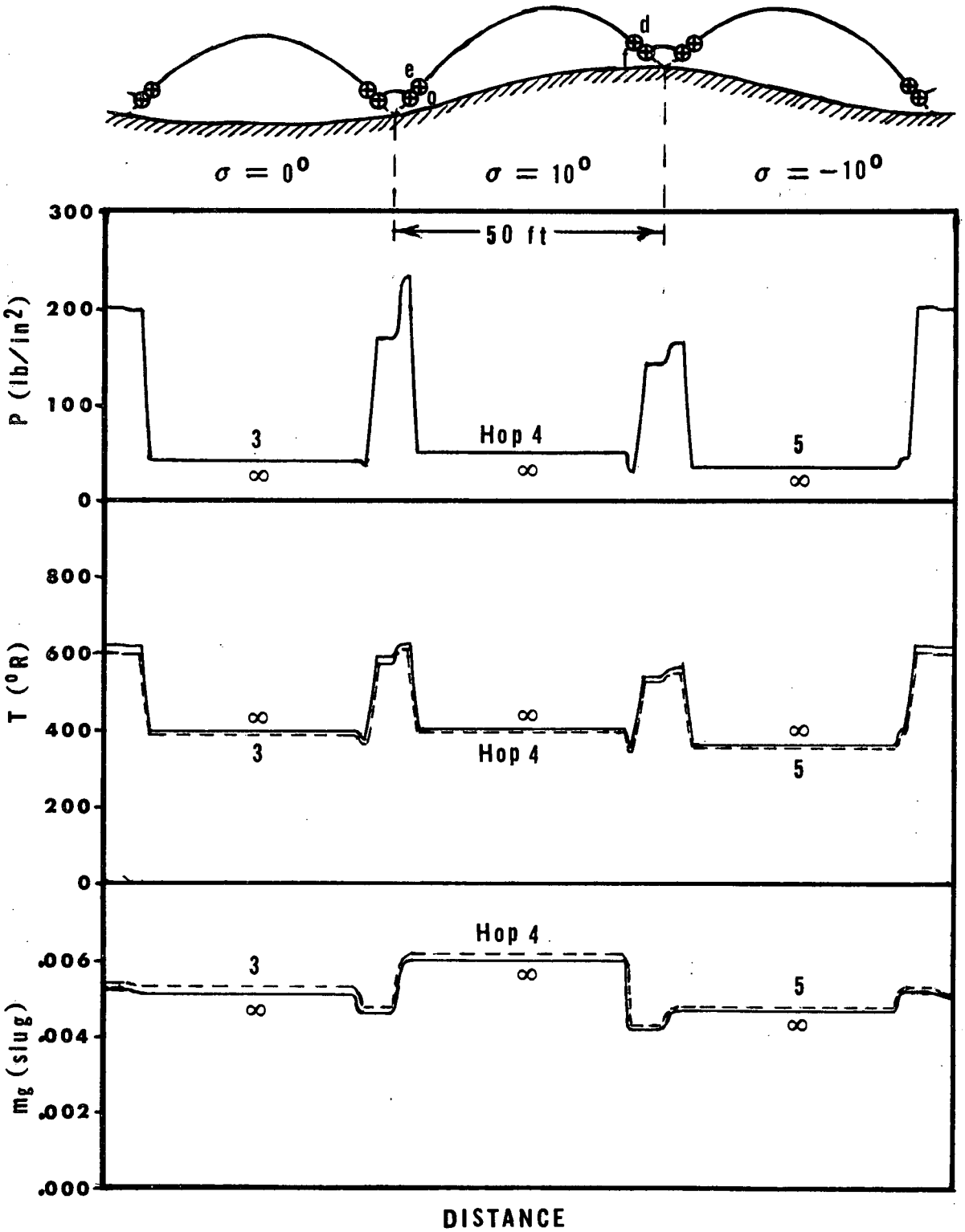

Figure 6. Variation of Gas State Variables and Mass during Repeated Hops

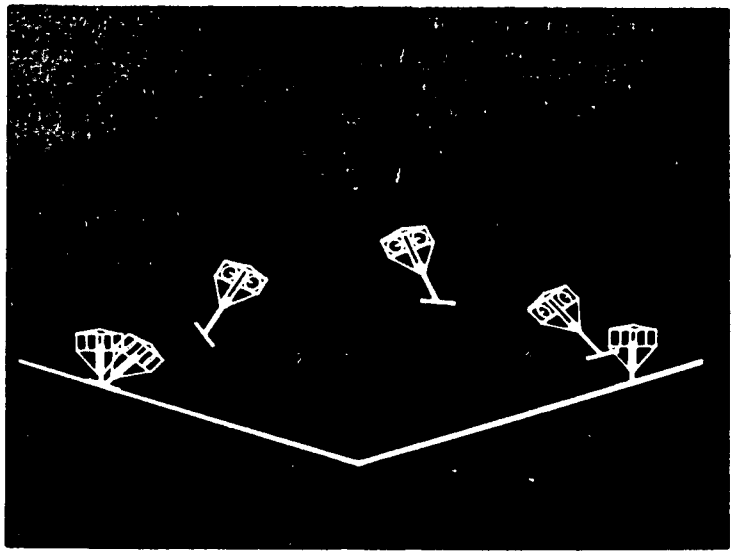

Figure 7. Multiple Exposure of Hopper Flight Simulation Displayed on Cathode Ray Screen

Section 5

TERRESTRIAL PROTOTYPE

In this section, a terrestrial technology demonstrator for the concept of lunar transportation is described. Establishment of preliminary design criteria, design, fabrication, and testing are summarized. The work described in this section is presented in greater detail in [13]. The demonstrator is shown in Fig. 8. A schematic of the various systems of the demonstrator is shown in Fig. 9.

The propulsion system provides the thrust required for trajectories ranging up to a 5 ft. vertical hop and a 10 ft. horizontal hop. Maximum length horizontal hops are obtained by using a 45° launch angle and straight line operating range of the vehicle is extended by repeated horizontal hops. Thrust forces are obtained by using compressed nitrogen at 600 psia to drive a piston down the 30" long cylinder that is located in the center of the structure. The piston shaft is attached to a cleated foot which presses against the ground to propel the vehicle. Hop trajectories with vertical, 67°, and 45° launch angles are achieved by reorienting the thrust cylinder. A hop is initiated by manually operating a momentary contact switch which activates an electrical circuit. As the switch is pressed the circuit transmits a timed electrical pulse to a three way solenoid valve. The valve opens a port which allows the high pressure nitrogen into the thrust cylinder. Pressure on the piston rapidly increases forcing the foot against the ground and accelerating the vehicle up the piston shaft.

When the piston has traveled 1 ft. it passes a set of blowout ports which dump the pressure into the atmosphere. The electrical circuit is preset to shut off the nitrogen at that time and vent the upper portion of the cylinder to atmosphere. Acceleration ceases and the vehicle enters flight. As the piston passes the blowout ports it contacts a compression spring which brings the relative velocity between the thrust leg and the vehicle to zero and then expands to thrust the leg back

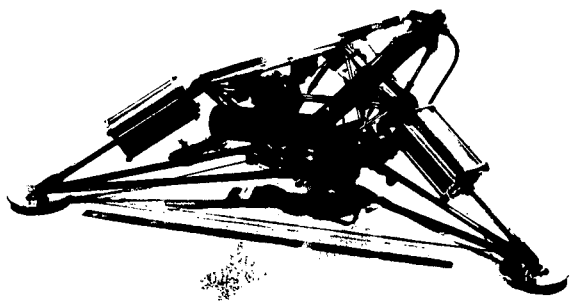

Figure 8. Technology Demonstrator

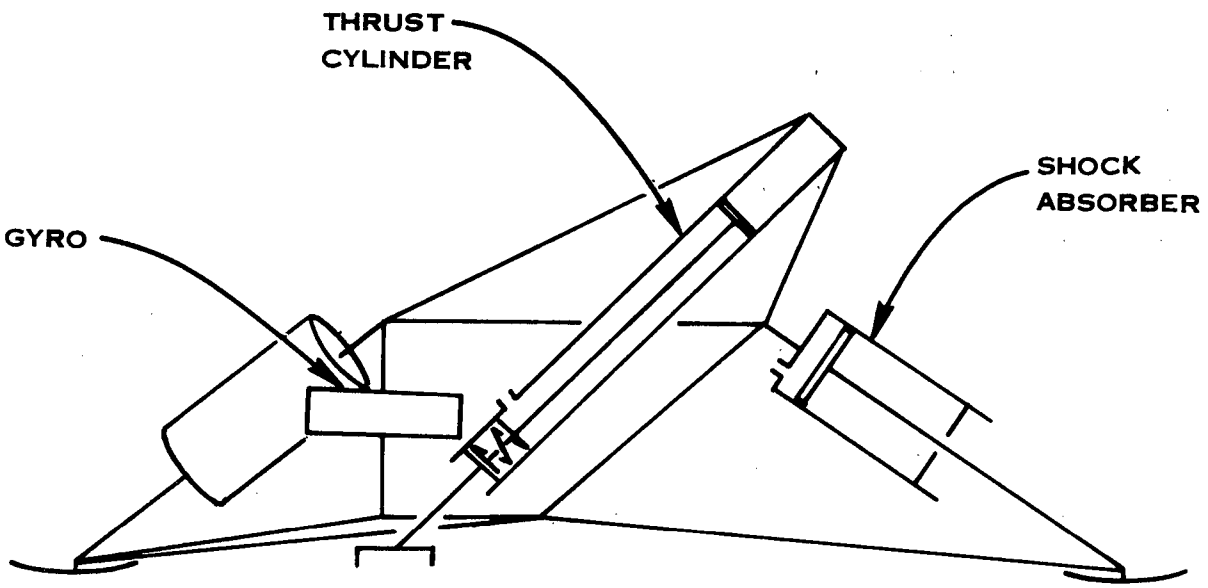

Figure 9. Systems Schematic for Technology Demonstrator

towards the launch configuration. It is held at the top of the cylinder by a weak extension spring so that it will not be bent during landing. The pressure available to the thrust cylinder is regulated from 2000 down to 600 psia which limits maximum acceleration to 15 g's to protect the stabilization gyro bearings. This also provides the constant upstream pressure required for repeatable hop trajectories. Variable hop heights are achieved by adjusting an orifice which controls the gas flow rate into the thrust cylinder and by controlling the interval during which gas is admitted. The cleated foot was designed to prevent slippage under the thrust required for 10 ft. horizontal hops. A mathematical model was used to determine component sizes. A vertical test rig was built and used to obtain control settings for different trajectories.

The gyro mounted in the rear triangle of the central structure is used to provide the torque required to cause a limited angle of precession about the vertical axis if impulsive torques are applied during launch. Thus the vehicle is stabilized to prevent continuous pitch or roll which could result in tumbling at touchdown. A mathematical model was developed and used to predict the relationship between thrust offset, gyro angular momentum and the resultant angle of precession or tilt. The gyro, which was recovered from a Norden bombsight, can provide stabilizing torques to limit the tilt angle to 15° if the thrust offset is held to a maximum of .125 in. during a maximum thrust 5 ft. vertical hop.

Although the lunar hopper design studied in this research used the same leg for both launching and landing, the terrestrial demonstrator used separate shock absorbers for deceleration. This was done to simplify vehicle attitude control requirements. Three large symmetrically located pneumatic cylinder shock absorbers and associated bottom linkage and radiused feet make up the landing gear. The symmetric configuration illustrated can tolerate any angle of rotation about the vertical axis at touchdown. The bottom leg of the linkage is long enough to insure that even if the coefficient of friction

reaches unity and the vehicle is tilted 15° at touchdown the landing force vector will compress the fully extended shock absorber. The 1 ft. vertical stroke of the propulsion system is the same as used in the landing gear and results in a 6 in. shock absorber piston stroke.

The kinetic energy of the vehicle is dissipated by compressing atmospheric air inside the shock absorber and accelerating it through an orifice in the cylinder head. A mathematical model of that process was developed [13] and used to determine the minimum piston diameter and associated orifice size required for the 5 ft. maximum hop height. Several piston sizes were arbitrarily selected and an optimum orifice area for each was obtained by maximizing the energy absorbed or minimizing the velocity at final impact. An apparently unique solution which would decelerate the demonstrator to zero velocity at final impact was obtained with a 2.5 in. diameter piston and a .125 in. diameter orifice. However, that solution produced deceleration forces in excess of the 15 g's that the gyro could tolerate. Therefore, the piston size was increased to 4 in. which resulted in decelerating the demonstrator to zero velocity earlier in the stroke and then allowing slow acceleration and final impact at a low velocity.

Each time vertical drop height is changed, the orifices are readjusted to achieve minimum velocity at final impact. The shock absorbers, initially contracted, must fully extend during launch to provide the required energy absorption capability. Although the inertial forces generated during launch were sufficient to overcome the friction forces which would prevent shock absorber extension, even a small adverse pressure differential working on the piston area of over 12 sq.in. could seriously hinder the required motion. Therefore, suction on the piston head was immediately relieved by a specially designed large floating wafer check valve which was installed in the cylinder head. Shock absorber extension took place almost as quickly as ground clearance occurred during takeoff.

The design of the central structure is controlled by various requirements of the propulsion, stabilization, and landing gear systems.

Minimum weight, simplicity of fabrication, and ease of analysis were accepted as basic requirements. The skewed triangle configuration provides an open central area for the required mounting and adjustment of the thrust cylinder, symmetric mount points for the landing gear, and balanced mounting areas for the stabilization and propulsion system components. The upper members of the structure were made long enough to provide rough adjustments in the gas bottle locations for center of gravity adjustment during initial assembly. Height of the structure is governed by the space required to mount the gyro in the rear triangle. Welding jigs were simplified by making the gyro and air bottle mount triangles vertical. Thrust cylinder reorientation is achieved by installing different sets of upper struts for each of the three hop trajectories. The length of the struts can be changed to locate the thrust foot location and provide for adjustment of the line of thrust application to reduce impulsive moments applied during launch.

The asembled vehicle is about 2 ft. high, 4 ft. between landing gear feet, and weighs 58 lbs. Fig. 10 illustrates the demonstrator in flight. Vertical hops of over 5 ft. and horizontal hops of over 11 ft. have been conducted with no stability or structural problems. Repeated horizontal hops can be used to extend the straight line operating range to over 150 ft.

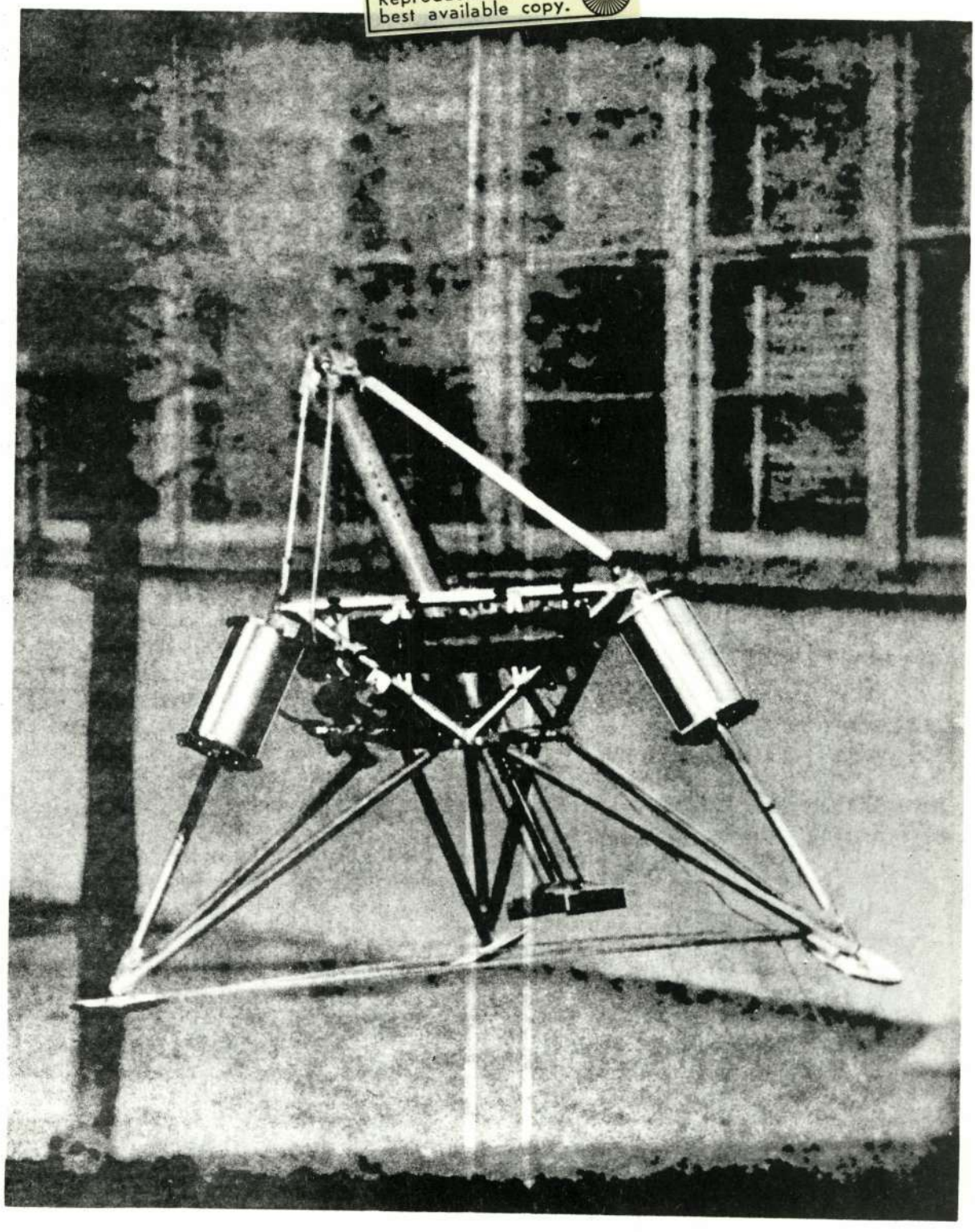

Figure 10. Terrestrial Demonstrator in Flight

Section 6

AUTOMATED HOPPING DEVICES FOR LUNAR EXPLORATION

Introduction

Current planning for manned space flight does not include lunar flights beyond Apollo 17. Surface mobility aids will be limited to "first generation" roving vehicles, but advanced transporters will not be developed until manned lunar flight becomes active again. To maintain exploration activities a vigorous automated program will be required. An essential tool in such a program is a remotely controlled surface equipment transporter. The USSR already has a roving device, Lunokhod [14], and the U.S. has proposed similar vehicles for many years [15]. Exploration missions to both the near- and far-side will be of high priority. A relay satellite stationed about the L_2 Lagrange point in a halo orbit can provide continuous communications between the lunar far-side surface and Earth [16]. Unmanned missions produce special problems of control, navigation, and guidance. Furthermore, a one-way mission does not permit sample return.

The optimum device for automated surface mobility is one that can use the lunar environment and peculiar operating situation advantageously. A hopping vehicle has inherent qualities of speed and fuel efficiency. It can view surface features with some elevation advantage while hopping and can stop at any desired site to collect data. Efficient use of fuel permits high range capabilities and electrical power can be used primarily for communications and instrument operation. Such a device can make visual observations, transmit data, and deploy instrument selectively. Basic operational aspects and possible configurations are discussed here.

Operational Aspects

Unmanned surface devices present special problems involving deployment, control, and guidance. The first hop would be vertical for surveying the local area and locating an initial landing site on a traverse. Propulsion parameters are then adjusted accordingly and a traveling hop is initiated. Take-off, ballistic, and landing are the three phases of each hop. Television cameras can supply continuous video information to earth-based operators. Two such operators will be required to perform guidance

and control functions on a continuous basis. There is a one-way time delay of up to 1.5 sec. due to the extreme distance between vehicle and operator. A further limiting factor is the picture transmission rate. However, it is assumed that sufficient power will be available for a fast data rate, because propulsion will not drain this source. Thus, the data transmission rate will be assumed sufficient to eliminate further delays in operation. Transmission distance and rate do severely limit the speed of automated rovers.

The profile of a typical hop permits delays to have only a minor effect on vehicle performance. Fig. 11 illustrates the sequence of events for remote operation. Operator 1 is responsible for take-off and landing phases while Operator 2 takes sightings and coordinates for future touch-down sites. During ballistic phase the attitude is automatically maintained. A hop is initiated when the"take-off" button is pushed. About 1.5 sec. later the thrust leg is released and motion commences. Operator 1 has no further duties until a landing decision must be made. An abort command can be given up to 1.5 sec. before actual surface contact. Rockets are used to perform abort maneuvers. Due to transmission delays, these rockets will be fired for about 3 sec. more than necessary for safe landing. Operator 2 uses part of the ballistic phase to look for landing sites for the following hop. He can start this about 1.5 sec. after the vehicle reaches suitable elevation for reconnaissance. When a site is selected its direction and distance are automatically recorded and propulsion parameters computed and sent up to the hopper by the end of the current hop. The ballistic phase is typically several seconds long and sufficient for reconnaissance and site selection. Each hop can span 50 - 100 feet, thus permitting high average speeds.

Configuration Considerations

The unmanned terrestrial demonstrator has been built and successfully flown to prove stability of attitude control and test performance capabilities. Much of the technology developed is directly applicable to unmanned hopping devices for exploration. Propulsion, stabilization, and vehicle dynamics are similar in principle and design for either manned or unmanned devices. Significant differences occur in guidance, navigation, and control, as is the case with lunar rovers. However, elimination of the human factors

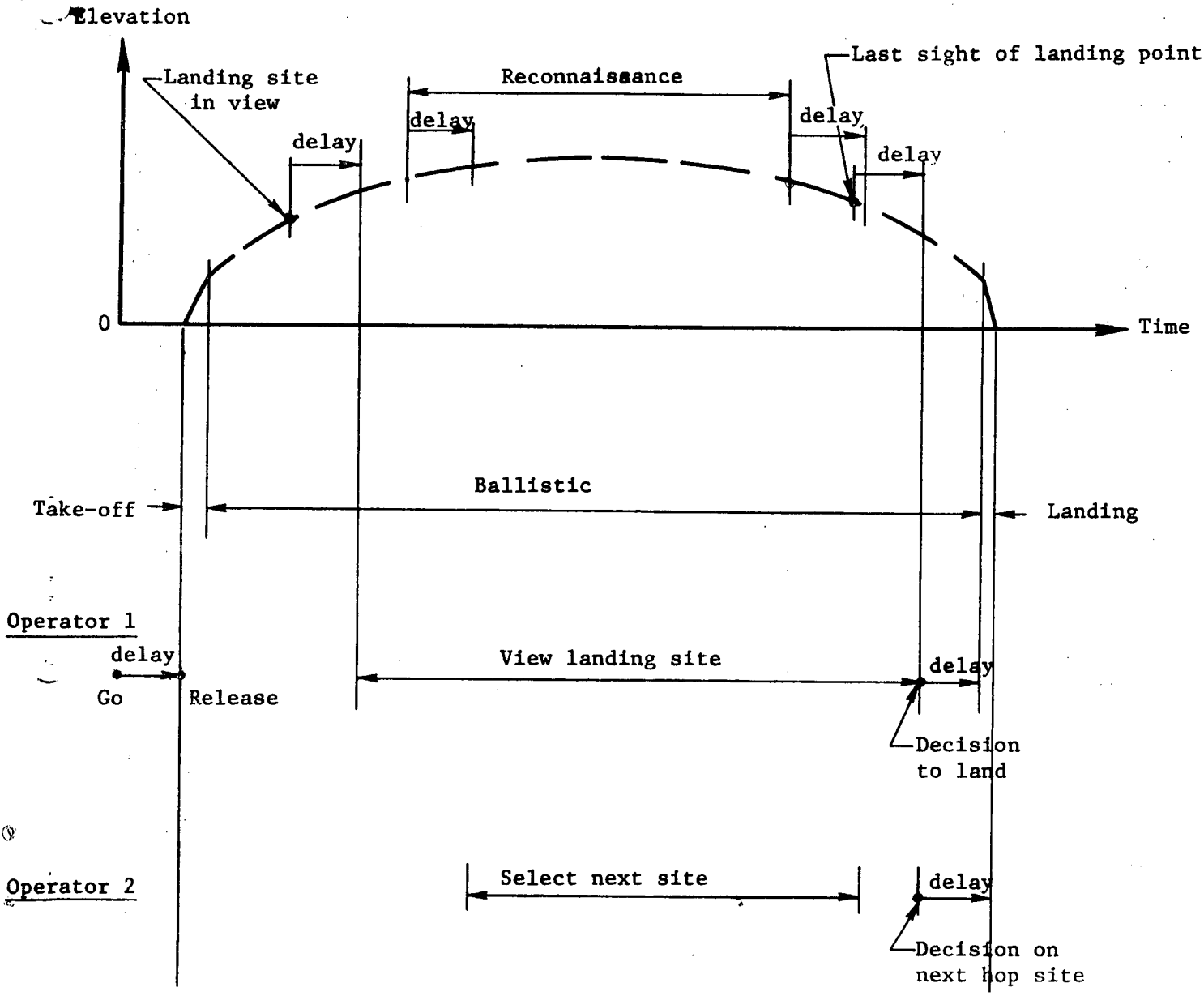

Figure 11. Remote Sequencing and Functions

restrictions permits increased hopper performance, because take-off and landing accelerations can be higher.

Rover performance is severely limited by the requirement for continuous surveillance of lurain while traveling from point to point, but remote operators on earth require surveillance from hoppers only part of the traveling time. Scientific instrument packages for either rover or hopper should have about the same weights. However, an unmanned hopper needs no wheels or large electric motors and requires much less electrical power for locomotion. An attitude control and abort system is needed for hoppers. Thus, both types of vehicles may have comparable weights.

A candidate unmanned hopper is illustrated in Fig. 12. This concept differs from the terrestrial demonstrator in that it has all required sub-systems for remote operation and incorporates two thrust leg mechanisms.

Each leg is used for alternate hops, i.e., the leg used for take-off is also used for landing but is idle during the next hop. During ballistic flight the legs rotate in opposite directions and exchange positions so that the idle leg is ready for the next hop as soon as landing is completed. Plane changes are accomplished with supporting leg mechanisms. The primary source of electrical power is an array of solarcells on the top dome. A radioisotope supply is used for maintaining instrument temperatures during lunar nights. Two television cameras are required for bifocal capability, and others may be desirable for on-site observations.

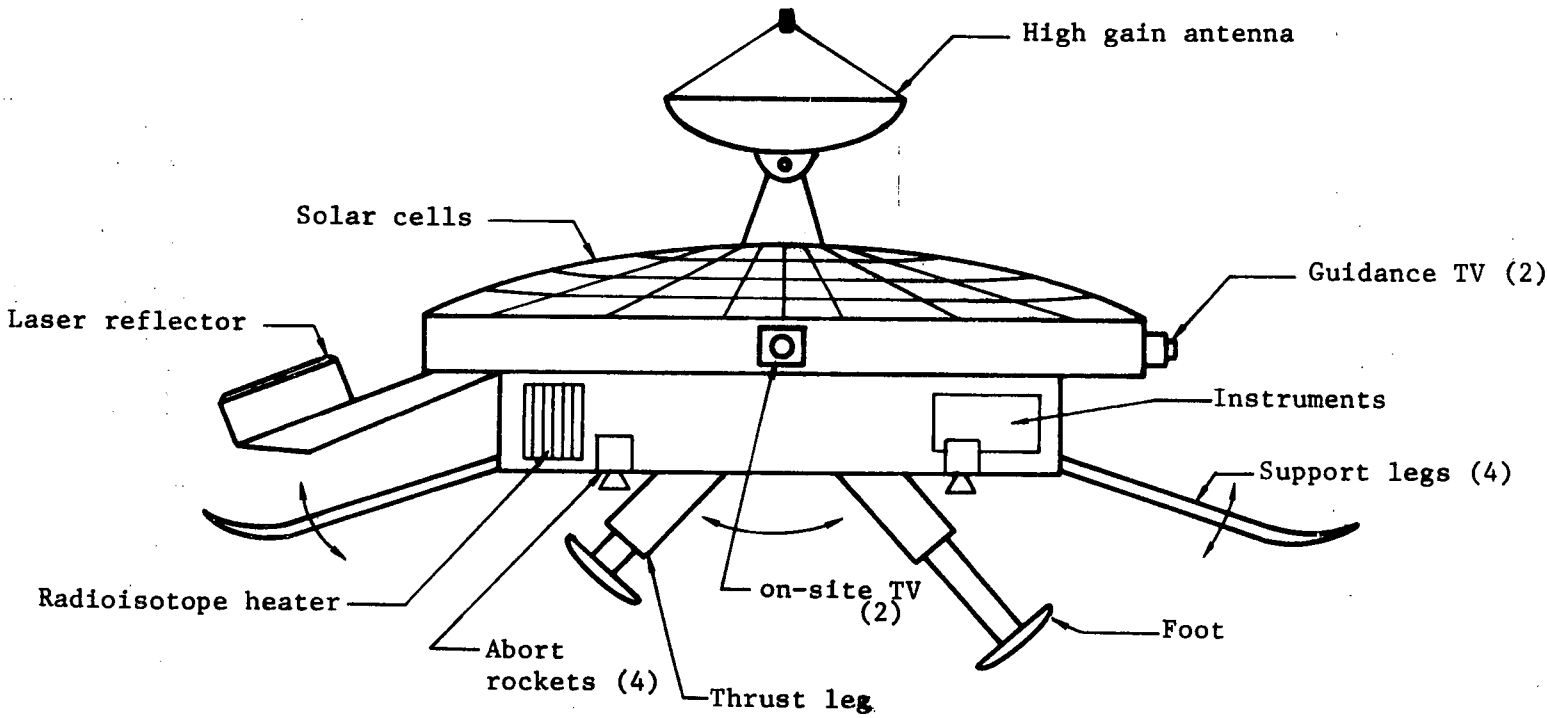

Figure 12. Candidate Unmanned Hopper Configuration

References

1. Seifert, Howard S., "The Lunar Pogo Stick," J. Spacecraft and Rockets, Vol. 4, No. 7, July,1967, pp. 941-943.

2. Kaplan, Marshall H., and Seifert, Howard S., "Hopping Transporters for Lunar Exploration," J. Spacecraft and Rockets, Vol. 6, No. 8, August, 1969, pp. 917-922.

3. Kaplan, Marshall H., and Seifert, Howard S., "Investigation of a Hopping Transporter Concept for Lunar Exploration," Department of Aeronautics and Astronautics, Stanford University, SUDAAR No. 348, June,1968.

4. Seifert, H., et al, "Small Scale Lunar Surface Personnel Transporter Employing the Hopping Mode," SUDAAR No. 359, Department of Aeronautics and Astronautics, Stanford University, September, 1968.

5. Seifert, H., et al, "Small Scale Lunar Surface Personnel Transporter Employing the Hopping Mode," SUDAAR No. 377, Department of Aeronautics and Astronautics, Stanford University, May,1969.

6. Seifert, H., et al, "Small Scale Lunar Surface Personnel Transporter Employing the Hopping Mode," SUDAAR No. 397, Department of Aeronautics and Astronautics, Stanford University, September, 1970.

7. Degner, Raymond L., "Effects of Cyclic Acceleration Pulses on Primates," Ph.D. dissertation, Mechanical Engineering Department, Stanford University, July 1971.

8. Gillies, J.A., ed., A Textbook of Aviation Physiology, Pergamon Press, Oxford, 1965, pp. 843-850.

9. Levy, Steven E., M.D., "Fat Embolism: An Important Cause of Morbidity and Mortality Following Trauma," The Journal of Trauma, Vol. 12, pp.3-31, October, 1970.

10. Lee, Richard A. and Pradko, Fred, "Analytical Analysis of Human Vibration," SAE Transactions, Vol. 77, Paper No. 680091, 1968.

11. Pasternack, Sam, Jr., "Attitude Control of Hopping Vehicles," Ph.D. dissertation, Department of Aeronautics and Astronautics, Stanford University, May, 1971.

12. Meetin, Ronald, "Propulsion and Ballistics of Lunar Hopping Vehicles," Ph.D. dissertation, Department of Aeronuatics and Astronautics, Stanford University, October, 1971.

13. Peterson, Stephen, "A Terrestrial Prototype of a Hopping Lunar Transporter," Engineers thesis, Mechanical Engineering Department, Stanford University, July, 1971.

14. Aviation Week and Space Technology, February 22, 1971, pp.22-23.

15. Wong, R.E., "Surface Mobility Systems for Lunar Exploration," SAE Paper 680373, presented at the Space Technology Conference, May 8-10, 1968, Washington, D.C.

16. Farquhar, R.W., "The Utilization of Halo Orbits in Advanced Lunar Operation," NASA-GSFC X-551-70-449, December 1970.